Development of forward osmosis membranes modified by cross-linked layer by layer assembly for brackish water desalination

Wafa Suwaileh[a], Daniel Johnson[a], Saeed Khodabakhshi[b] Nidal Hilal[a,c*]

[a]*Centre for Water Advanced Technologies and Environmental Research (CWATER), College of Engineering, Swansea University, Swansea, SA1 8EN, UK*

[b] *Energy Safety Research Institute, Swansea University, Bay Campus, Swansea, SA1 8EN, UK*

[c] *NYUAD Water Research Center, New York University Abu Dhabi, Abu Dhabi, UAE*

Abstract

Membranes having high water flux and minimum reverse solute flux at low operating pressures are the ideal membranes for the forward osmosis (FO) process. In this work, we report the use of a LbL surface modification strategy to fabricate a novel positively charged FO membranes. The main purpose of this work was to fabricate an effective selective layer onto a commercial PES ultrafiltration membrane, which functioned as a support layer, to provide the best performance for treatment of brackish water by FO. The new membranes containing a mixing ratio of 0.1 MPDADMAC: 0.001 MCMCNa in the polyelectrolyte complex exhibited the best performance in terms of minimum reverse solute flux and acceptable water flux as compared to that for membranes containing a mixing ratio of 0.1 MPDADMAC: 0.01 MCMCNa. The improved performance and physicochemical properties of the new membranes were explored by various analytical techniques and were compared to the pristine membrane. Firstly, structural characterization revealed that the new selective layer was homogenous, uniform and strongly adhered to the substrate resulting in excellent water permeability and acceptable reverse solute flux. Secondly,

it was found that the optimal curing temperature was 60 ^{O}C for 4 hours that contributed to enhanced membrane performance. Lastly, the developed ranking protocol was adopted to optimize the membrane performance in terms of the water permeability coefficient (A) and solute permeability coefficient (B). According to this optimization procedure, the best performing membrane was membrane coated 2.5 bilayers which had water permeability and solute permeability coefficients of 23.1 L m^{-2} h^{-1} bar^{-1} and 1.54 L m^{-2} h^{-1} respectively.

Keywords: Forward osmosis, surface modification, layer by layer assembly, polyelectrolyte complex, optimization, Modeling

Highlights

1. Layer by layer surface modification increases membrane surface hydrophilicity.
2. Modification produced membrane with good water flux and minimal reverse solute flux.
3. Model determined optimal curing temperature and time for LBL modification.
4. 2.5 bilayer membranes had high water and low solute permeability coefficients.

Email addresses: n.hilal@swansea.ac.uk (Nidal Hilal)

1. Introduction

The production of fresh water from saline water resources, including seawater and brackish water is an essential to meet the increasing global fresh water demand [1]. Traditional thermal desalination technologies are effective at providing fresh drinking water from saline water resources but have high energy requirements leading to high production costs. Alternatively, the forward osmosis process (FO) is an emerging technology that is able to purify saline water resources and separate salts efficiently with less impact on the environment and high economic efficiency [1]. However, the crucial challenges in the FO process are those related to the development of the draw solution and choosing a membrane suitable for the process [2].

Membrane fouling is an unavoidable issue in almost all membranes based filtration processes. However, membrane scaling is considered as the bottle neck that increases the operation cost and the cost of fresh water [3]. Therefore, to improve FO membrane productivity, chemical alteration has been reported in several earlier studies.

Chemical alteration is an easy method which involves applying an antifouling coating to the membrane surface or by altering the surface chemical groups. The main reason for this is to change the surface properties and decrease the affinity of salt components or foulants to the membrane surface. For example, to develop a negatively charged nanofiltration (NF) membrane, different methods have been proposed, such as treatment with photo-radiation [4], low temperature plasma [5], chemical cross-linking, and layer by layer (LbL) assembly [6]. Among these procedures, the layer-by-layer (LbL) procedure has been performed to prepare an ultrathin and uniform separation layer without complicated manufacturing processes through alternate deposition of polycation and polyanion polyelectrolytes on the substrate surface [7, 8]. The advantages of this method are related to its easy operation, flexibility, controllable film thickness and good hydrophilicity compared to conventional chemical modification strategies [7]. For instance, Qiu [9], used this approach to fabricate an NF-FO

membrane to achieve maximum rejection of Mg^{+2} ions. This charged membrane showed superior selectivity while the water flux declined due to the thick selective layer formed from six multilayers. Liu [10], prepared a PVDF-FO membrane through depositing multilayers of polyethylenimine (PEI) and sodium alginate (SA) on polydopamine layer. Similarly, the thickness of this film influenced the water permeability whilst the reverse solute flux decreased. Wang [11] used the LBL method to fabricate an Aquaporin Z (AqpZ)-incorporated double-skinned FO membrane that exhibit good hydrophilicity due to the strong bond between water molecules, acidic COO^-, and amine groups on the PSS-terminated double skinned (T-PSS) substrate. In FO experiments using DI-water feed and 2M $MgCl_2$ DS, the water flux was 13.2 LMH, whilst the reverse solute flux was 3.2 g m^{-2} h^{-1}. Moreover, to evaluate the antifouling properties of FO membranes when using 200 ppm sodium alginate foulant, Salehi [12] used layer by layer method to incorporate positive chitosan (CS) and negative graphene oxide (GO) nanosheets in the polyamide selective layer. This novel membrane showed the best antifouling tendency as compared to other TFC membranes. Nevertheless, the new FO membrane having 10 LBL bilayers produced low water permeation and remarkably low reverse solute flux in the presence of 1M sucrose or 1M Na_2SO_4 as the DS solution and DI-water as the FS solution. This might be due to a trade-off between water flux and reverse solute flux. Gonzales [13] proposed a novel LBL method by coating the PVDF-PAA nanofiber support layer with polyethylenimine (PEI) and PAA to construct a polyelectrolyte layer underneath the polyamide selective layer. The hydrophilicity and porosity of the novel membrane were significantly improved resulting in superior water permeation and low structural parameter of 221 μ m. The water flux was recorded as 37.8 and 45.2 LMH and the reverse solute flux as 4.5 and 4.9 g m^{-2} h^{-1} when using 1.5 M NaCl and 2.0 M NaCl as the DS and DI-water as the FS. A recent study on LBL assembly explored the influence of MPD and TMC concentrations and the deposition cycles on the membrane separation performance [14]. It was found that the ideal FO membrane achieved water flux of 14.4 LMH as well as relatively high solute reverse flux of 7.7 g m^{-2} h^{-1} during the FO experiment utilizing 1M NaCl as the DS and DI-water as the FS. However, the LBL method needs special properties of the thin film with a minimal number of layers to

reduce the production cost and fabrication time.

The chemical cross-linking procedure to fabricate charged NF membranes was also employed. Some of the advantages of this crosslinking method is easy to scale up, has lower cost, and requires less preparation time. A facile procedure of homogeneous polyelectrolyte complex membranes (HPECMs) was reported in the literature [15, 16]. This method provides a homogenous continuous thin selective layer and controlled cross linking degree of the polyelectrolytes as well as better water permeation. Ji [16] synthesized a charged NF membrane using this method to improve the rejection of inorganic salts and organic species. It was found that the modified membrane exhibited an excellent water flux, salt rejection with various valence, antifouling properties against organic species, and good stability during long term operation.

Generally, the structure of the polymeric membrane depends on the preparation conditions. Mathematical modeling can be used to set design guidelines for the membrane productivity based on the relation between the fabrication parameters and final membrane performance. For instance, Tsay [17] proposed a theoretical model to relate the effects of mass transfer processes during phase separation on the membrane structure. The polymer film composition at the precipitation instant was chosen as a useful indicator of skin and sublayer structures, to identify conditions leading to sponge-like and finger-like morphologies. However, the reliability of applying this model is questionable as many of the parameters used in the model were unavailable for every system. Therefore, there is an urgent need for a methodology to optimize the fabrication parameters to develop membranes with controlled performance. Here, a simple relational equation between the water permeability coefficient (A) and the solute permeability coefficient (B) was adapted for ranking the best performing membrane for selecting the optimal preparation conditions. This method has not been used previously, and it would help in selecting the best fabrication conditions for various types of membranes, especially for the development of large-scale commercial FO membranes.

In this work, a combination of HPECMs method and the LBL method is introduced for the first time

in this research, to fabricate a positively charged NF- FO membrane, aiming to enhance the water flux and the reverse solute flux. Manufacturing a positively charged NF membrane was expected to enhance the selectivity for divalent over monovalent cations, thereby rejecting scale precursors from feed solutions and mitigating scaling. The effect of curing temperature and time on the membrane performance was investigated. The tailored FO membranes were characterized extensively with several analytical techniques and using laboratory-scale FO system. The obtained results revealed that the new NF membranes produces a good stability and improves FO membrane performance, especially by achieving a low reverse solute flux value. Finally, a previously developed ranking protocol for determining the optimum water permeability coefficient (A) and the reverse solute permeability coefficient (B) for the tailored membranes was used.

2 Experimental

2.1 Materials and chemicals

Commercially available flat polyethersulfone (PES) ultrafiltration membranes (UP150T) were obtained from Microdyn-Nadir GmbH, Germany. The UF membrane has an asymmetric structure that is composed of a polyester backing material and PES selective layer. They were used as the substrate for the layer by layer modification. These membranes have a molecular weight cut-off (MWCO) value of 150,000 Daltons, thickness of 210-250 mm, and high water permeability of 285 LMH/bar (data provided by the manufacturer).

All the chemicals were ACS grade accredited and were procured from Sigma Aldrich (Merck). Poly (diallyl dimethyl ammonium chloride) (PDADMAC) (Mw= 70,000 g/mol, 20% aqueous solution) was used without further purification and poly (sodium 4- styrenesulfonate) (PSS, Mw = 70,000 Da) was used as the respective polycation and polyanion for LBL assembly. Sodium carboxymethyl cellulose (CMCNa) was dried in a vacuum oven at 60°C. Sodium hydroxide (NaOH) and hydrochloric acid (HCl) were analytical reagents. Deionized water was produced from a water

purification system (Millipore) and used for preparation of the polyelectrolytes and utilized as the feed solution.

2.2 Method

2.2.1 Preparation of layer by layer-modified PES membranes

2.2.2 Substrate preparation

Prior to the modification, a pretreatment process was applied to the PES substrate. The pristine substrates were immersed in deionized water for one hour followed by soaking in 25% concentration (v/v) 2-propanol solution for another hour, and then were stored in in deionized water overnight. Prior to LBL modification, the membrane was soaked in 2.0 M NaOH solution at 45 ^{O}C for one hour to hydrolyze and causes negative charges to accumulate on the PES substrate surfaces [8].

2.2.3 Preparation of polyelectrolyte complex

The procedure of Ji [16] was employed to synthesize the CMCNA and PDADMAC (PEC) with some alterations. An illustration of the modification protocol is demonstrated in Fig.1. PDADMAC was selected as it is a strong polycation and is capable of ionic complexation with anionic polyelectrolyte CMCNa. The positive charges of this polyelectrolyte were expected to remain permanent on the substrate at pH value <6 where the polyelectrolyte would be less protonated [18] . The polyelectrolyte complex was prepared using a 250 mL of CMCNa and PDADMAC dissolved in 0.009 mol/L HCl solution as a protonated reagent. The mixing ratio between CMCNa and PDADMAC was varied, where two mixing ratios of 0.1 $M_{PDADMAC}$: 0.01 M_{CMCNa} and 0.1 $M_{PDADMAC}$: 0.001M_{CMCNa} were chosen.

Next, a dropwise addition of the PDADMAC solution into CMCNa using a burette was

performed, whilst the mixture was stirred at 800 rpm until the end of reaction. During the addition of the PDADMAC solution, a turbidity in the mixture was observed due to macroscopic phase separation. After adding the whole PDADMAC solution, a white precipitate insoluble in water was formed indicating the end of the reaction. The ionic complexation between both the PDADMAC and the CMCNa occurred when the endpoint was reached, thereby the crosslinking between the PDADMAC and the CMCNa was successful. At the end, the white precipitate was separated from the mixture using a centrifugal separator at 12,000 rpm and 25 ^{o}C for 20 minutes. This precipitate was then dried in a vacuum-oven at 60 ^{o}C for 24 hours. The solid material obtained was dissolved in the NaOH solution. Normally, the mole concentration of the NaOH with different mixing ratio of MPDADMAC: MCMCNa was determined based on this equation:

$$[NaOH] = [CMCNa] \times (1 - M_{PDADMAC} : M_{CMCNa}) \quad (1)$$

In which, [CMCNa] represents the mole concentration of the CMCNa monomer and was measured from the mass concentration of PECs and its $M_{PDADMAC}$: M_{CMCNa} [19]. A low concentration of NaOH was utilized to maintain a stable crosslinking between the PDADMAC and the CMCNa and to ensure that there were no free NaOH ions in the solution. The CMCNa was dissolved in HCl solution so that the ionization degree and charge density were reduced. Thus, low concentration of strong polycation (PDADMAC) was enough to neutralize CMCNa. As the PDADMAC is a strong polycation, it is expected that the positive charges will be predominant in the PEC solution. Moreover, the concentration of NaOH was calculated based on the ionic complexation degree (ICD) equation. Accordingly, the value of MPDADMAC was equal to that for MCMCNa which means all the positive charges chains on PDADMAC undergone ionic interaction with all the negative charges chains on CMCNa. In principle, the PEC solution is almost free of NaOH ions and there was no chance for the interaction between

OH^- ions of NaOH and ions of the PDADMAC. Besides, the pH of the PEC solution was ≈ 8 which confirms that the solution was almost free of NaOH ions [19]. Finally, the PEC solution was deposited on the substrate as the primary material and the positively charged layer on the negatively charged PES substrate.

As the UF membrane is known to be highly porous, a denser and tighter ~~slightly thicker~~ selective layer is preferable to fabricate a tight membrane needed for achieving a minimal reverse solute flux. In comparison with earlier studies [~~12~~ 16], the mixing ratio of polyelectrolytes was varied and the modification cycles in this research was optimized to form a nonporous selective layer. A CMCNa polyelectrolyte was incorporated into the PDAMAC polyelectrolyte to form inherent cross-linking and ensure permanent stability on the substrate. It was expected that this method would allow fabrication of a stable selective layer with minimal bilayers based on an LBL protocol. More importantly, the time of the LBL synthesis route could be minimized, and a low cost of the production strategy could be achieved.

Moreover, for the success of the interaction and binding of the PEC on the substrate, PSS was introduced as a negatively charged polyelectrolyte, leading to a good adherence to the substrate. A further reason for using PSS was to enhance the hydrophilicity and homogeneity of the substrate, as CMCNa is hydrophobic by nature. The migration of a carboxyl functional group into the substrate is important to produce a stable ionic bonding with the polycation and the surface. Saren [~~24~~20] postulated that the presence of hydrophilic carboxyl functional groups on the membrane surface would result in a hydrophilic substrate.

It is crucial to explore the optimum curing temperature and time for the modified membrane without affecting the intrinsic properties of the selective layer. The temperature was varied from 50-70 ^{o}C and the time ranged from 30 minutes to 4 hours. Within this context, it is essential to select the most suitable preparation conditions to promote the membrane interstice transport parameters.

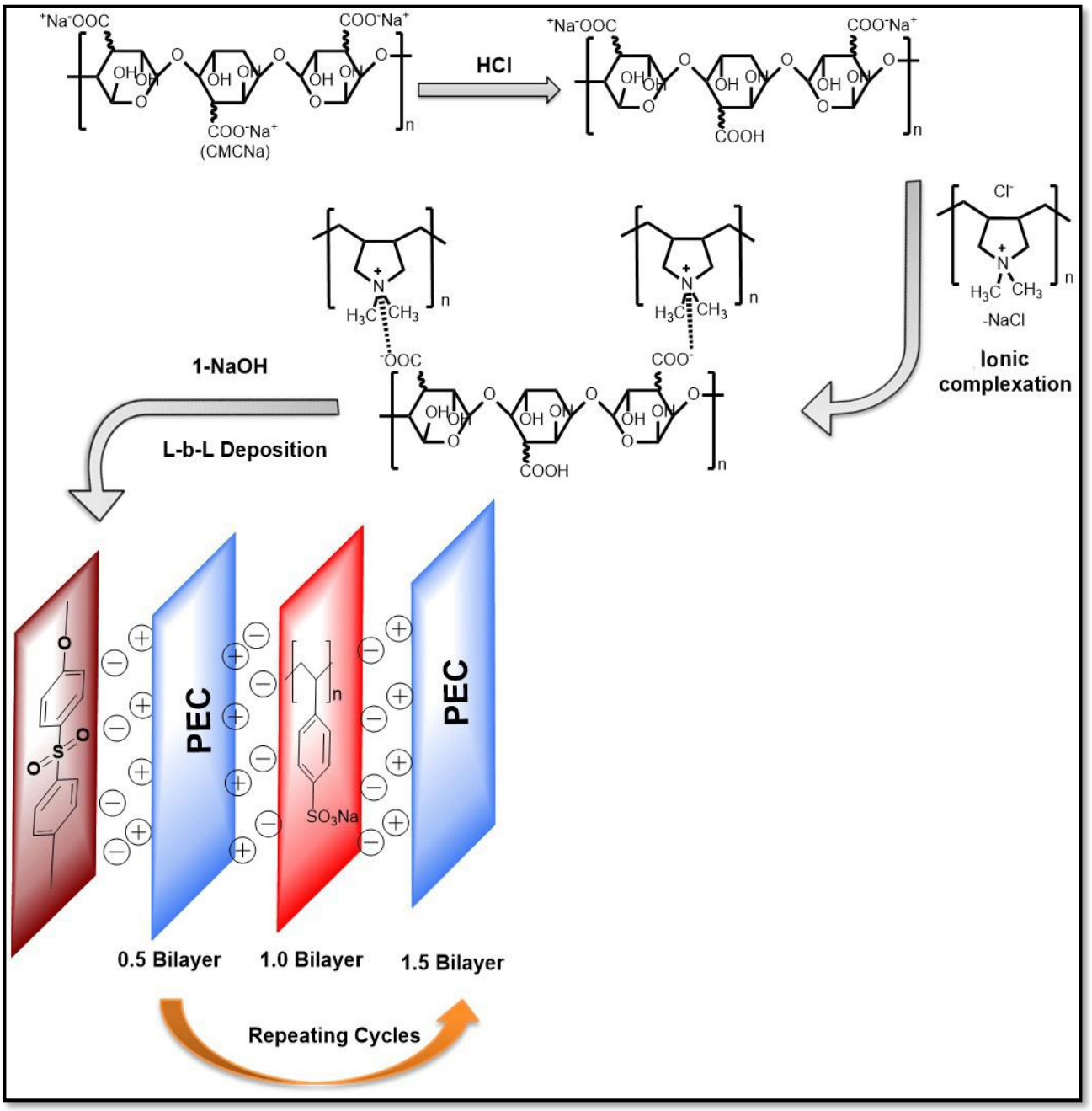

Figure.1: Schematic illustration for the synthesis process of the HPEC and LBL assembly on the PES membrane.

2.2.4 Layer by layer assembly

The LBL modification involves the alternate adsorption of the polycation (PEC) and the polyanions (PSS) as shown in Fig.1. It is worth noting that PSS was selected because it is a strong polyanion with a pKa value of 1.0 [18]. PSS was dissolved in 0.2 mol/L sodium chloride at a concentration of 0.1 g L^{-1}. The pH was 5.8 and 8.0 for the PSS and the PEC respectively. The LBL protocol for fabricating a selective layer is outlined in Fig.1. A custom-made frame was used to make certain that polyelectrolyte multilayers were built up on the negatively charged substrate of the PES membrane. The negatively charged PES substrate was first dip-coated in PEC solution for approximately six hours to ensure the adsorption of the PEC solution. The membrane was then subjected to thermal treatment at 60 ^{O}C for four hours followed by another four hours at 60 ^{O}C in vacuum. The substrate was then rinsed with 0.2M NaCl solution (pH 5.7) followed by immersion of the substrate in the PSS solution for six hours. The membrane was again soaked in PEC solution for six hours followed by the thermal treatment in oven at 60 ^{O}C for four hours followed by another four hours at 60^{O}C in vacuum. The first trilayer $(PEC/PSS/PEC)_1$ was formed on the PES substrate. The deposition route was conducted to form three bilayers on the PES substrate for each mixing ratio of polyelectrolytes. For example, membrane coated-PEC layer denoted 0.5 bilayer, membrane coated-PEC/PSS layers denoted 1.0 bilayer, and membrane coated-PEC/PSS/PEC layers denoted 1.5 layer and so on. The membranes were denoted as follows: PEC1-0.5 – PEC2-1.5 – PEC3-2.5.

After the deposition cycle, the membranes were soaked in 15 wt% glycerol solution for four hours to preserve the membrane structure and were then dried overnight under ambient condition [21, 22]. Prior to the filtration experiments, the membranes were stored in DI water.

2.1 Membrane substrate porosity, mean pore size and structural parameter (S)

The structural parameter (S), was calculated from the porosity and the average pore radius using the following relation [23]:

$$S = \frac{\tau\, t_s}{\varepsilon} \qquad (2)$$

where, τ, t_s, and ε are the sub-layer thickness, tortuosity and porosity respectively. The overall porosity (ε%) was determined by gravimetric analysis, measuring the mass difference of wet (m1, g) and freeze-dried sample (m2, g). The densities of water (ρ_w) and polysulfone (PS_f) (ρ_p) are 1.00 and 1.37 g/cm3, respectively. The tortuosity is related to the porosity and described as:

$$\varepsilon = \frac{(m_1 - \frac{m_2}{\rho_w})}{\frac{m_1 - m_2}{\rho_w} + m_2/\rho_p} \text{ X } 100 \qquad (3)$$

$$T = \frac{(2-\varepsilon)^2}{\varepsilon} \qquad (4)$$

The average pore radius was calculated using the Guerout–Elford–Ferry equation:

$$r_m = \sqrt{\frac{(2.9-1.75\varepsilon)\times 8\eta l Q}{\varepsilon \times A_m \times \Delta P}} \quad (5)$$

In which η corresponds to the water viscosity of 8.9 x 10^{-4} Pa s, l is the membrane thickness measured from SEM cross-sections, Q is the volume of water permeate per unit time (m s^{-1}), A_m and P are the effective membrane area (m^2), and the applied pressure of 1 bar respectively.

2.2 Membrane characterization

Surface and cross-section structures of the pristine and modified membranes were observed using a field-emission scanning electron microscopy (SEM) instrument coupled with energy-dispersive X-ray spectroscopy (EDS) (Hitachi high technologies corporation, Japan) [24]. All samples were sputter coated with platinum to improve the conductivity of the surface before the examination.

The functional groups and chemical structure of pure and synthesized PEC products, pristine membrane, and the modified membranes were characterized using an attenuated total reflectance Fourier Transform Infrared Spectroscope (ATR-FTIR, Shimadzu UK Ltd, UK) [25]. Spectra were recorded from 500 to 4000 cm^{-1} with 60 scans.

Contact angle measurements were carried out using the sessile drop technique (Fibro DAT 1100, Sweden). The captive bubble method was conducted using a J-shaped needle filled with DI water to produce an air bubble on the inverted immersed membrane surface in a water bath [26].

Zeta potential of the pristine and modified membrane surfaces was analyzed by an ElectroKinetic Analyzer (EKA, Austria) [27]. Streaming potentials were determined using an asymmetric clamping cell connected to this analyzer at pH 5.5 in 10 mM NaCl. The pH of this

solution was adjusted in the range of 3.0 – 9.0 by adding drops of 0.1 mol/L NaOH or 0.1 mol/L HCl. 6 streaming potential measurements were recorded at each pH value.

2.3 Membrane intrinsic parameters in FO system

Pure water permeability and reverse solute flux were measured using a lab-scale crossflow FO filtration system that is described in our previous work [23]. To determine the water permeability coefficient (A) and solute permeability coefficient (B), the method developed by Tiraferri [28] was employed. DI water was used as a feed solution and various concentrations (0.5, 1.0, 1.5, 2.0 mol/L) of NaCl aqueous solution were used as the draw solution. The water flux was measured from the slope of the below function:

$$J_w = \frac{\Delta V}{A_m \times \Delta t} \quad (6)$$

Where, ΔV (L) is the volume change of the DS over a predetermined time, Δt (h) and A_m is the effective membrane area.

The concentration of NaCl in the DS and FS was measured using a standard conductivity curve plotted using solutions of known concentration. The reverse solute flux (J_s) was then calculated from [29]:

$$J_s = \frac{(C_e V_e) - (C_o V_o)}{A_m \Delta t} \quad (7)$$

Where C_e is the salt concentration in the FS (g L^{-1}) and C_o is the initial salt concentration in the FS (0 g L^{-1}). V_e is the final volume of the FS (L) obtained after time Δt (h), while V_o denotes the initial volume of the FS (L).

2.6 Ranking model development

Three different membranes (PEC1-PEC2-PEC3) having a mixing ratio of 0.1 MPDADMAC: 0.01 MCMCNa and three membranes (PEC1-PEC2-PEC3) having a mixing ratio of 0.1 MPDADMAC: 0.001MCMCNa were fabricated based on the LBL procedure. The water flux and reverse solute flux of these membranes were obtained using the FO system using DI water and 4 different concentrations of NaCl as a DS. Then, the A and B values of all these membranes were calculated via the typical FO theoretical model.

In our earlier research we developed a mathematical method which considers the water flux and reverse solute flux values to determine the optimum water permeability coefficient (A) and solute permeability coefficient (B), which are the crucial parameters in FO system [30]. This model involves using second-order differential equation to calculate the optimum value of A and B. The below equation reflects the second-order linear differential equation [31]:

$$y'' + p(x)y' + q(x)y = f(x) \quad (8)$$

By plotting values of A against values of B, an equation was obtained:

$$A = -0.499B^3 + 6.6423B^2 - 24.019B \quad (9)$$

Using direct linear differentiation, the optimum values of A and B can be obtained. Firstly, differentiation was applied to find out the optimum B value that minimized the value of A using:

$$\frac{dA}{dB} = 0 = -3 * 0.499B^2 + 2 * 6.6423B - 24.019 \quad (10)$$

Two mathematical values for B are obtained, while only the positive value was considered. The optimum value of A was obtained from the first step in eq.9.

The A and B values calculated based on these mathematical equations support the identification of the best performing FO membrane. Therefore, the preparation conditions of this membrane was chosen as the optimal preparation conditions for the curing temperature, curing time, and mixing ratio of polyelectrolytes for the surface modification procedure. Overall, this method allows the selection of the best membrane to achieve the optimal A and B values as it will be fabricated based on the optimal preparation conditions.

3 Results and discussion

3.1 Analysis of PEC product

ATR-FTIR was performed to probe the chemical functional groups of the PEC product. The spectra of pure products including mixing ratio of 0.1 M_{PDAMAC}: 0.001 M $_{CMCNa}$ and 0.1 M_{PDAMAC}: 0.01 M_{CMCNa} are shown in Fig.2A. According to the previous study [25], very similar peaks were observed, such as the broad band centered at 3259 and 3370 cm^{-1} that were ascribed to the hydrogen bonding OH stretching region. While the small peaks at 2898 and 2920 cm^{-1} might be attributed to C-H stretching along with the ring methane hydrogen atoms. The stretching vibration at 1589.2, 1591.5 cm^{-1} was derived from the existence of the carboxyl group (COO-). Additional OH stretching bands in-plane and attached C-H groups in CMC were noticed at 1414.2 and 1416.6 cm^{-1}. Also, the

characteristic bands at 1059 and 1028 cm^{-1} can be assigned to C-O stretching on polysaccharide skeleton. Major differences, however, were found at wave numbers of 1319, 1322.4, 896.7, and 806 cm^{-1} as compared to the pure CMCNa material. Accordingly, these peaks can be only corresponded to the alkyl groups in the polymeric chain of PDADMAC [32, 33]. This implies a complete crosslinking between PDAMAC and CMCNa.

3.2 Membrane substrate characterization

3.2.1 Chemical structure of PEC-coated substrate

Chemical characterization of the pristine and modified PEC membranes was performed by means of ATR/FT-IR. Fig.2B displays the spectra for the pristine sample, CMCNa coated-substrate, and all modified PEC membranes. It can be seen that the coexistence of absorption bands at 1043 cm^{-1}, which is the characteristic band for CH_2 bonded in the structure of CMCNa [33]. The sample shows the characteristic band of carboxylic acid groups, which appeared at 1642.8 cm^{-1} [16] suggesting the presence of (COONa). However, a slight shift of this peak to 1642.8 cm^{-1} is apparent, which was due to lower concentration of the HCl solution than monomer concentration of this polyelectrolyte. The presence of this ionized carboxylic group is due to the successful crosslinking between PDADMAC and CMCNa which binds via ionic interaction and their charges [15]. Moreover, a broad intense hydroxyl peak appeared at 3413 cm^{-1} [33].

To further elucidate the ionic cross-linking structure of PECs, Fig.2-B depicts spectra for each bilayer of PEC-1, PEC-2, and PEC-3. The adsorption bands at 628.95, 626.38, and 623.49 cm^{-1} for all samples can be directly ascribed to the presence of alkyl groups in the polymeric chain of PDADMAC. In addition, it was observed that the intensity of the peak at 1642.8 cm^{-1} increased with the addition of polyelectrolyte multilayers, can be ascribed an increased proportion of protonated carboxyl groups during the preparation of the acidic solution. The characteristic bands appeared at 1040.5, 1043.17, and 1045.6 cm^{-1}, probably corresponded to the stretching vibrations of the

sulfonate groups [32], indicated the presence of sulfonic species impregnated into the PEC layer. Furthermore, all bilayer spectra show a broad intense peak around 3300-3500 cm^{-1} assigned to hydroxyl group bands due to grafting of CMCNa to the PDADMAC [33]. The above results confirmed the presence of the polyelectrolyte coating layers on all the PES substrates.

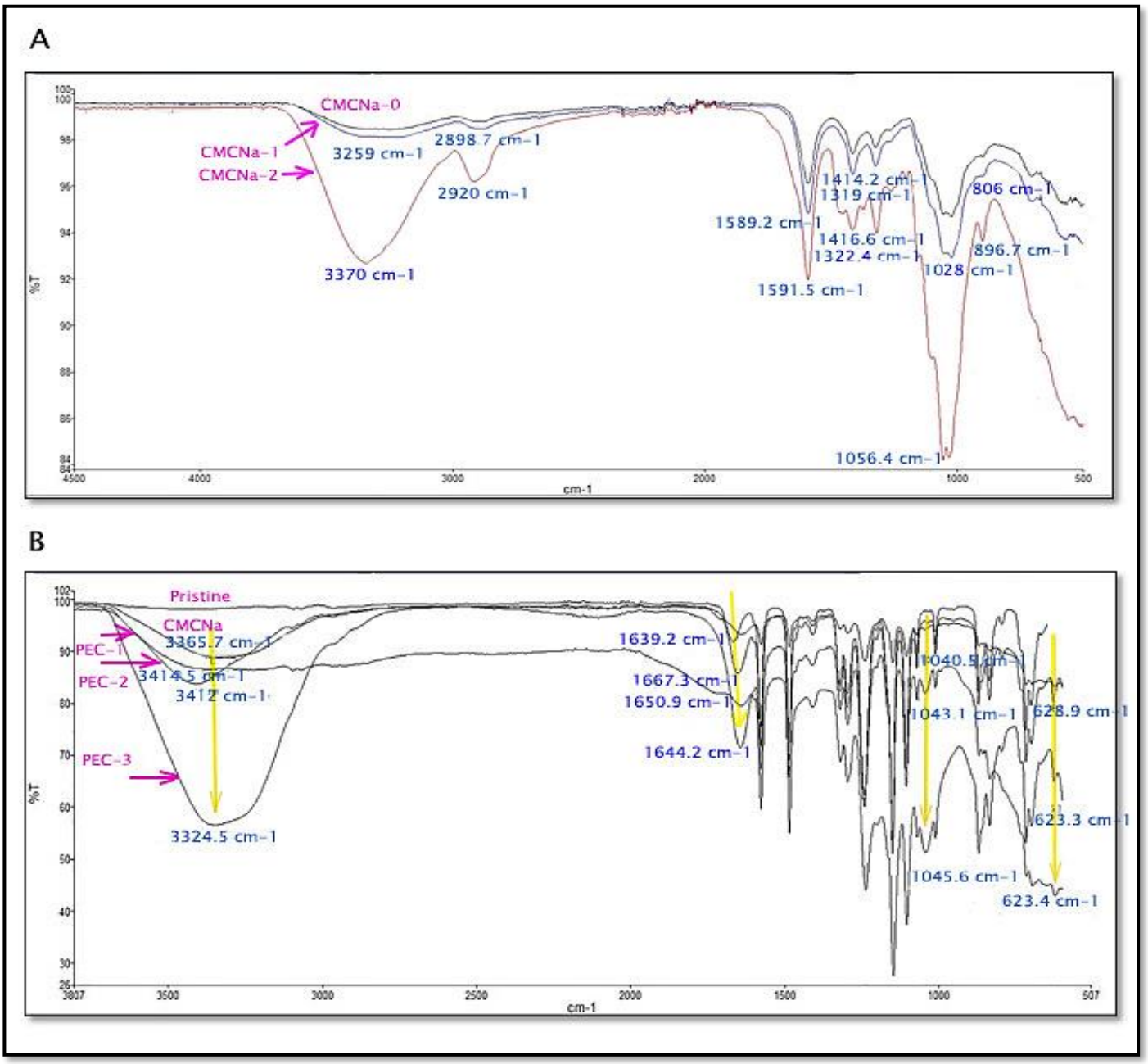

Figure.2: (a) Spectra of pure CMC (black) and PEC synthesized product with mixing ration of 0.1 M_{PDAMAC}: 0.001 M_{CMCNa} (blue) and 0.1 M_{PDAMAC}: 0.01 M_{CMCNa} (red). (b) Spectra of pristine substrate and those of the LBL assembly with mixing ration of 0.1 M_{PDAMAC}: 0.01 M $_{CMCNa}$ (PEC-1, PEC-2, PEC-3).

3.2.2 Membrane substrate morphologies

Surface and cross-section of the pristine and modified membranes were observed by SEM. Fig.3A-B-C showed the membrane composed of typical asymmetric porous microstructure. Fig.3A-B shows that the surface was covered in a thin and highly porous PES layer with a thin skin layer on the top. The porosity of the support layer as calculated from equ.2 was 65%. The high porosity was formed from the diffusion of water into the film and the mixture of water and polar solvent such as N, N′–dimethylformamide (DMF) diffusing out of this film creating large micropores during phase inversion [34]. It can be observed that the average thickness of the ultrathin skin layer was approximately 30.1 μm (see Fig.3B). The mean pore radius of the PES support layer was quantified by equ.4 corresponds to 83.2 nm.

When the first PEC layer was deposited on the substrate, there were some tiny aggregates formed. These aggregates were probably produced due to the crosslinking reaction that happened in the PEC. Another reason is the highly porous substrate which may allow the viscous polyelectrolyte to penetrate the sublayer pores. It is clear from Figs.3D that the surface uniformity was enhanced, and the film structure was improved upon the deposition of more 2.5 bilayers. It appeared to have a relatively smooth, even, and nonporous morphology and an average thickness of 12.0 μm. The surface structure comparable to that seen in a previous study [19]. This is because of the high mobility of the positive polyelectrolyte that is in contact with the negative polyelectrolyte, causing rearrangement reaction on a slower timescale. When the concentration of the coating polyelectrolyte was slightly increased, the solution density and charges density were also improved. Thus, the chain entanglements between PEC molecules were less aggregated and the hydrophilic coating layer was found to be strongly adhered on the surface. This enabled the formation of a thicker, uniform and defect free skin layer on the porous PES substrate. Fig.3E-H shows the thickness of the final selective layer for each mixing ratio and the porosity of the sublayer after modification. It can be seen that the selective layer

was thicker for the membrane coated with 2.5 bilayers containing 0.1 M_{PDAMAC}: 0.01 M_{CMCNa}. Alongside, there was no significant difference between the microstructure of the sublayer for pristine and the altered membranes as shown in Figure.3F-I.

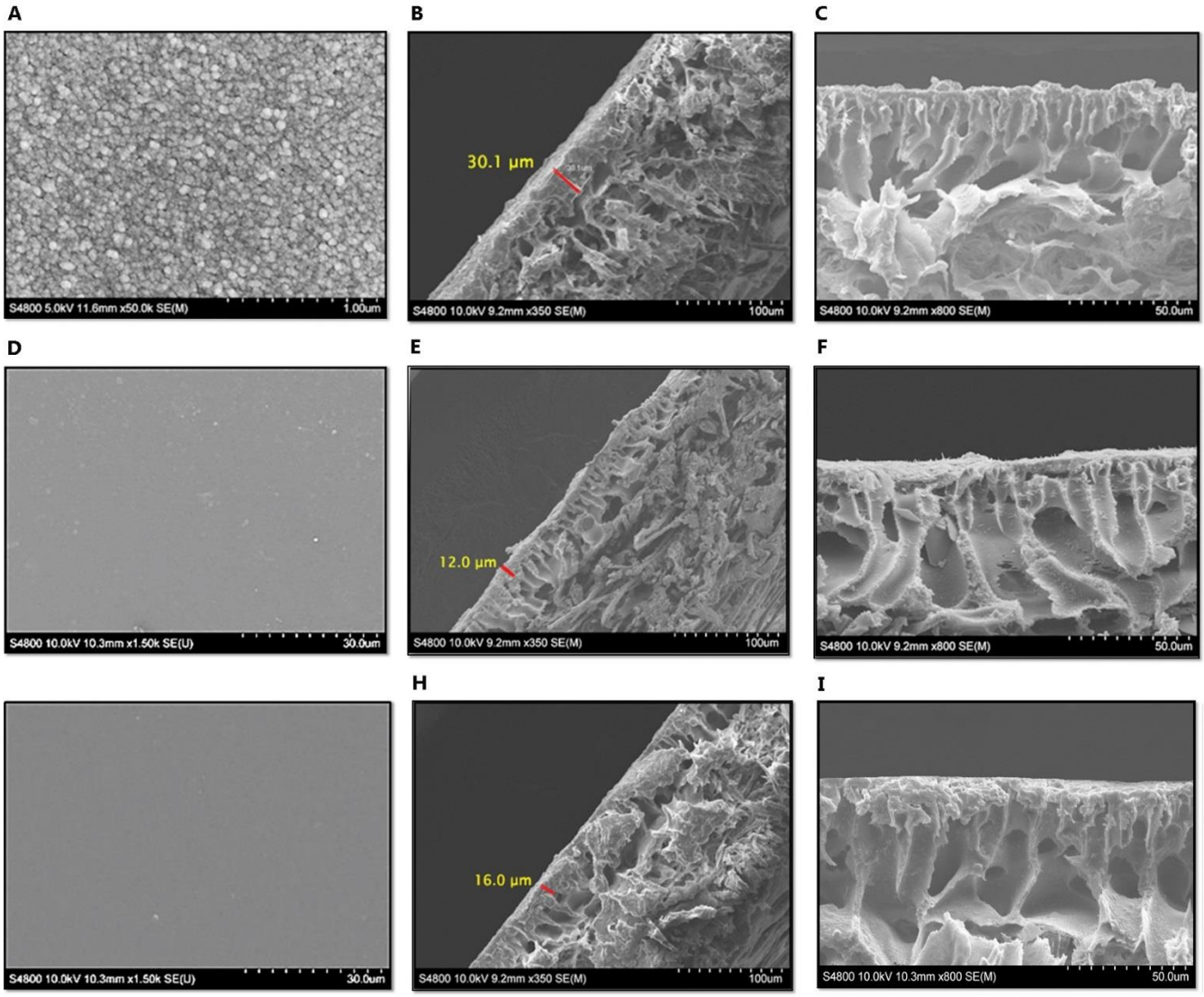

Figure.3: (a, b, c) surface morphology and porosity of the pristine membrane, thickness of the sublayer is 30.1 μm, and finger like structure of the sublayer respectively. (d, e, f) Surface morphology, the thickness of the selective layer is 12 μm and the same sublayer structure for the membrane-M1. (g, h, i) Surface morphology, thickness of the selective layer is 12 μm and the same sublayer structure for the membrane-M2.

3.2.3 Membrane substrate hydrophilicity

Table.1 illustrates the results of water contact angle measurements. It was observed that both pristine and altered membranes exhibited a hydrophilic nature (i.e. contact angles < 90°). The initial contact angle of the pristine membrane was about 60.4° which indicated moderate wettability. All the altered membranes had a smaller contact angle, which was decreased by 30% after depositing 2.5 bilayers as shown inTable.1. It was expected that the reduction in contact angle and excellent hydrophilicity would improve the membrane performance in terms of low fouling tendency and good water permeability. In comparison with the pristine membrane, the high hydrophilicity of the modified membrane can be attributed to the excess of the hydrophilic functional groups such as –OH and $-SO^{-3}$ in CMCNa and PSS polyelectrolytes respectively, which had higher water solubility. It was reported that incorporating a negatively charged polyelectrolyte including ionizable species, such as carboxyl and sulfonic groups, can increase hydrophilicity on the membrane surface [35]. During the coating process, there was a strong interaction between the hydrophilic polyelectrolyte and membrane surface, which allowed many free COONa groups and OH groups to migrate toward the substrate and increase its hydrophilicity. As a result, the contact angle of PSS layer on the substrate was around 41.3°. Moreover, the PEC is inherently ionically cross-linked, and the cross-linking degree was controlled during the preparation process. Therefore, a smooth and uniform surface of the modified membranes was produced which may have enhanced the contact angle measurements.

Table.1: Summary of contact angles of pristine and modified membranes with both mixing ratios. M1 indicates 0.1 M_{PDAMAC}: 0.001 M_{CMCNa} and M2 indicates 0.1 M_{PDAMAC}: 0.01 M_{CMCNa}.

Mixing ratio	Membrane	Contact angle
	Pristine	60.4°
M1	PEC-1	58.9 °
	PEC-2	52.9 °
	PEC-3	46.4 °
M2	PEC-1	49.2 °
	PEC-2	32.8 °
	PEC-3	30.6 °

3.2.4 Effect of the positively charged coating on substrate zeta potential

The influence of PEC on the substrate charge was investigated by applying multilayer polyelectrolytes of PEC, with results presented in Table.2. The PES substrate was negatively charged, with higher negativity over the acidic pH range [36]. It can be seen inTable. 2, the zeta potential was more positive over the pH range 4-9, for one PEC bilayer compared to pristine membrane. It is most likely that the positive charges of PEI coating shielded the negative charges of carboxyl groups on the PES substrate. This PEC bilayer coated-substrate showed the lowest zeta potential of 15.3 mV, when compared with the other modified membranes at a pH of 3.0. When depositing more PEC bilayers on the substrate, a higher zeta potential at the same pH value was achieved. This implies that the PEC coated substrate produced higher positive charges upon increasing the number of bilayers regardless of the mixing ratio between both the polyelectrolytes. The charge density increased when applying multilayer polyelectrolytes on the PES substrate. It can be suggested that during the ionic complexation, the positive charge on PDADMAC neutralized carboxylic acid charged groups COONa on CMCNa. Other preparation conditions may also influence the coating structure and ultimately the membrane performance.

Table.2: Zeta potential values of positively charged membranes with both mixing ratios at pH 3. M1 indicates 0.1 M_{PDAMAC}: 0.001 M_{CMCNa} and M2 indicates 0.1 M_{PDAMAC}: 0.01 M_{CMCNa}.

Mixing ratio	Membrane	Zeta potential
	Pristine	0.5
M1	PEC-1	15.3
	PEC-2	18.5
	PEC-3	21.9
M2	PEC-1	23.9
	PEC-2	29.4
	PEC-3	31.4

3.3 Effect of curing temperature and time on membrane productivity

The curing temperature can influence the water permeation and the reverse solute flux of the modified membranes. As shown in Fig.4A-B, when the curing temperature was increased from 50 °C to 60 °C for four hours each, the water permeation was slightly augmented from 24.1 LMH to 24.7 LMH using 1 mol/L NaCl as DS and DI water as FS, whilst the solute reverse flux decreased from 76.8 to 71.3 g/(m^2.h). This indicated that increasing the temperature to 60 °C would improve the solubility, diffusivity and crosslinking degree of the coating solution. This led to a thinner, more homogenous and contiguous selective layer on the substrate. The reverse solute flux was not changed upon raising the temperature to 70 °C, while the water flux showed a slight decrease. It should be pointed out that a prolonged curing time would affect the structure of the membrane surface and probably shrinkage of the micropores in the sublayer. Thus, the modified membrane was subjected to the optimum temperature of 60 °C for

approximately four hours, following previously reported procedure [16]. It can be concluded that the correlation between curing temperature, treatment time, and membrane productivity may be coincidental. This is because the thickness and integrity of the selective layer and the efficiency of the crosslinking degree are the most crucial parameters in determining the membrane productivity.

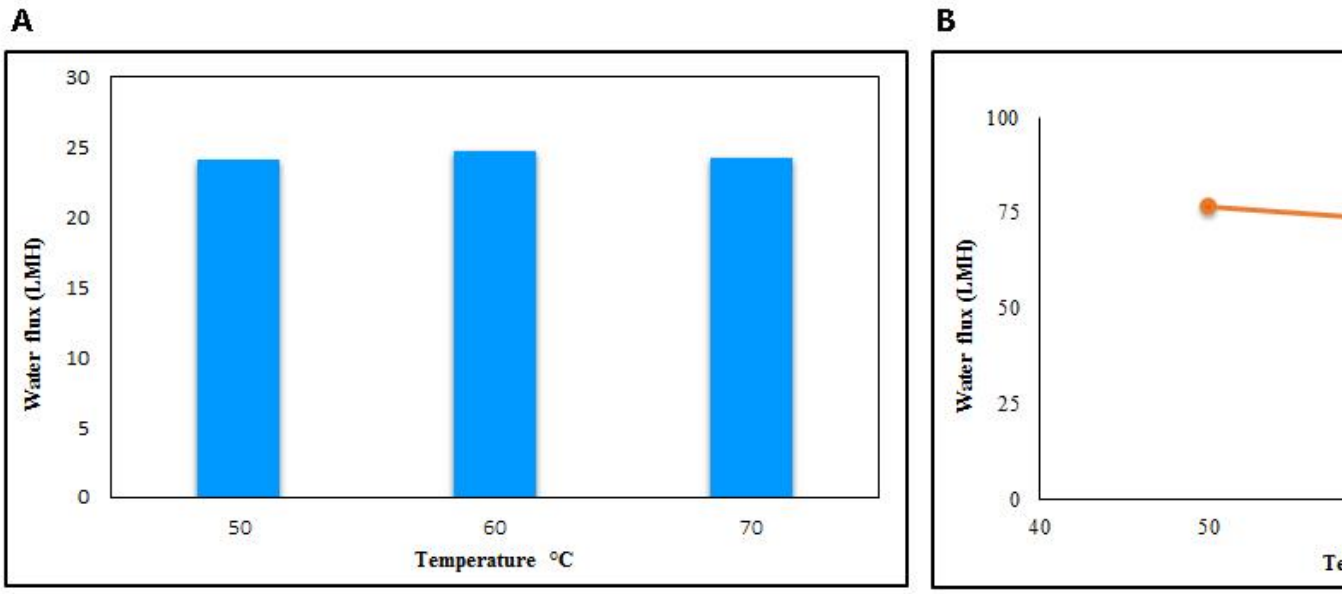

Figure.4 (a-b): Impact of various curing temperatures on the water flux and reverse solute flux.

3.4 Effect of multilayer polyelectrolytes on substrate porosity

Surface modification by polyelectrolyte may cause shrinkage of the inner pores in the substrate. These altered membranes exhibited a remarkable shift toward smaller mean pore size governed by the thickness of the coating layer and preparation time. The average pore size of the pristine and modified membranes is listed in Table.3. When a polyelectrolyte bilayer was added into the PES support layer, a minimal change in the average pore size was occurred. The average pore size was lowered to 74.6 nm as compared to pristine membrane having average pore size of 83.2 nm. In

contrast, there was a drastic decrease in the average pore size upon applying more polyelectrolyte bilayers on the substrate. It must be noted here that, there was a correlation between the mean pore size and the polyelectrolyte modification time. The data summarized in Table.3 indicated that an increase in the coating time resulted in a sharp drop in the mean pore size from 83.2 to 41.9 and 33.1 nm. Similar observations were made in a previous work [37]. This can be attributed to the adsorption of the polyelectrolyte in the inner pores which partially blocks some substrate pores and then creates a dense selective layer after four hours (see Fig.5). This can adversely affect the structural parameter (S) as it is inversely proportional to the porosity of the membrane sublayer [38]. Therefore, a reduction in the substrate porosity contributes to a larger structural parameter. S for membranes coated with 2.5 polyelectrolyte multilayers were very close in value at 1663.1 μm and 1688.8 μm for membrane containing 0.1 MPDADMAC: 0.001 MCMCNa and 0.1 MPDADMAC: 0.01 MCMCNa. Observation suggest that the polyelectrolyte penetrated in the entire pores of the sublayer and hence agglomerated. Not surprisingly, the influence of the (S) value at various draw solution concentration and preparation conditions introduced great hindrance of the solution mass transport within the sublayer. In contrast, a small structural parameter of the support layer is important to suppress the ICP effects in the FO experiments.

Table.3: Mean pore size of the pristine and altered membranes. M1 indicates 0.1 M_{PDAMAC}: 0.001 M_{CMCNa} and M2 indicates 0.1 M_{PDAMAC}: 0.01 M_{CMCNa}.

Mixing ratio	Membrane	Mean pore size (nm)
	Pristine	83.2
M1	PEC-1	74.7
	PEC-2	58.6

	PEC-3	33.1
M2	PEC-1	74.4
	PEC-2	61.9
	PEC-3	41.9

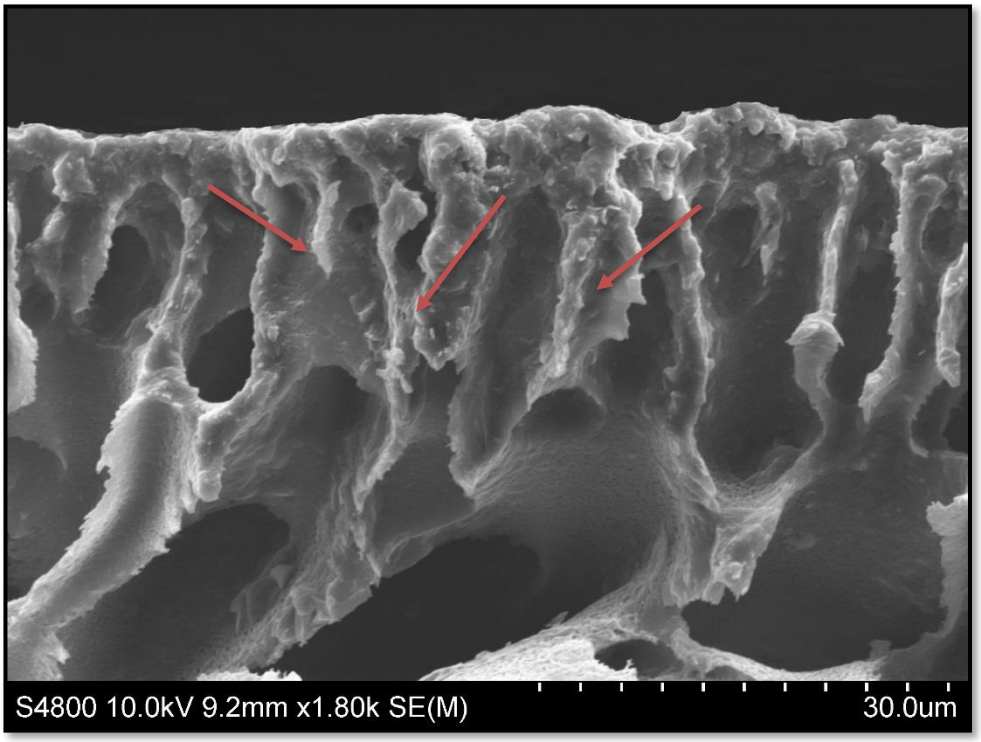

Figure.5: showing some of the polyelectrolyte solution trapped in the inner pores of the PES sublayer.**3.5 Membrane performance in FO system**

The overall productivity of the tailored membrane was assessed by the water flux and reverse solute flux (Fig.6). It was observed that the water flux and reverse solute flux were the highest with a bilayer coated- substrate (PEC-1) at mixing ratio of 0.1 M_{PDAMAC}: 0.01 M_{CMCNa} as compared to other altered membranes. Upon increasing the concentration of NaCl DS, the water flux and reverse solute flux became higher as it was challenging to avoid trade-off

between water flux and salt rejection. At a concentration of 2.0 mol/L NaCl DS, the water flux and reverse solute flux were remarkably reduced. The same observations were reported in earlier studies as the FO membrane was affected by a permeability–selectivity trade-off mechanism [15]. Furthermore, the coupled effect of a high porous support layer and large structural parameter of 905.8 μm further exacerbated the reverse solute flux from the DS into the FS causing a serious ICP to occur. This is a curious finding as the higher structural parameter would have accelerated the mass transfer resistance leading to serious ICP impacts [2]. This implies that a greater influence of the ICP resulted in a continuous drop in the water flux upon increasing the concentration of the draw solution. It is to be noted however that the polyether sulfone support layer is likely to have a high structural parameter which is the reason behind the decrease in the water flux for all the altered membranes in this work. Even though the ICP effect was severe, the inverse charge of the selective layer contributed remarkably in reducing the reverse solute flux while the water flux was comparable. The DS was permanently undergoing rapid dilution, to a significant extent. All these factors resulted in lower water permeation and low reverse solute flux for all the modified membranes with both mixing ratios of polyelectrolytes. In (Fig.6A-B), the water flux and reverse solute flux exhibited similar trends as the high water flux associated with high reverse solute flux at higher DS concentration ranged from 0.5 to 1.5 mol/L. According to Holloway et al. [39], the physical structure of the support layer can accelerate the diffusion rate of the solute from the DS to the selective layer resulting in high reverse solute flux when increasing the DS concentration.

When 2.5 bilayers were deposited on the surface, a noticeable decrease in the water flux and reverse solute flux was observed when using 0.5, 1.0, 1.5, and 2.0 mol/L NaCl as DS and DI water as the FS (see Fig. 6A-B). For membrane coated with 2.5 bilayers-M1, the water flux dropped from 19.8 to 14.1 LMH and reverse solute flux reduced from 70.1 to 40.0 g/(m^2.h) when utilizing 1 mol/L NaCl as a Ds and DI water as a FS.

An appreciable reduction in the water flux and reverse solute flux was also observed from 20.2

to 14.6 LMH and 52.4 to 30.3 g/(m².h) respectively for membrane coated 2.5 bilayers-M2 (see Fig.6C-D). Even though the ICP effect was severe, the inverse charge of the selective layer contributed remarkably in reducing the reverse solute flux while the water flux was comparable. Most recent studies have also highlighted similar findings [9, 10]. When increasing the number of coating layers on the substrate, a thicker selective layer was formed leading to reduced water permeation.

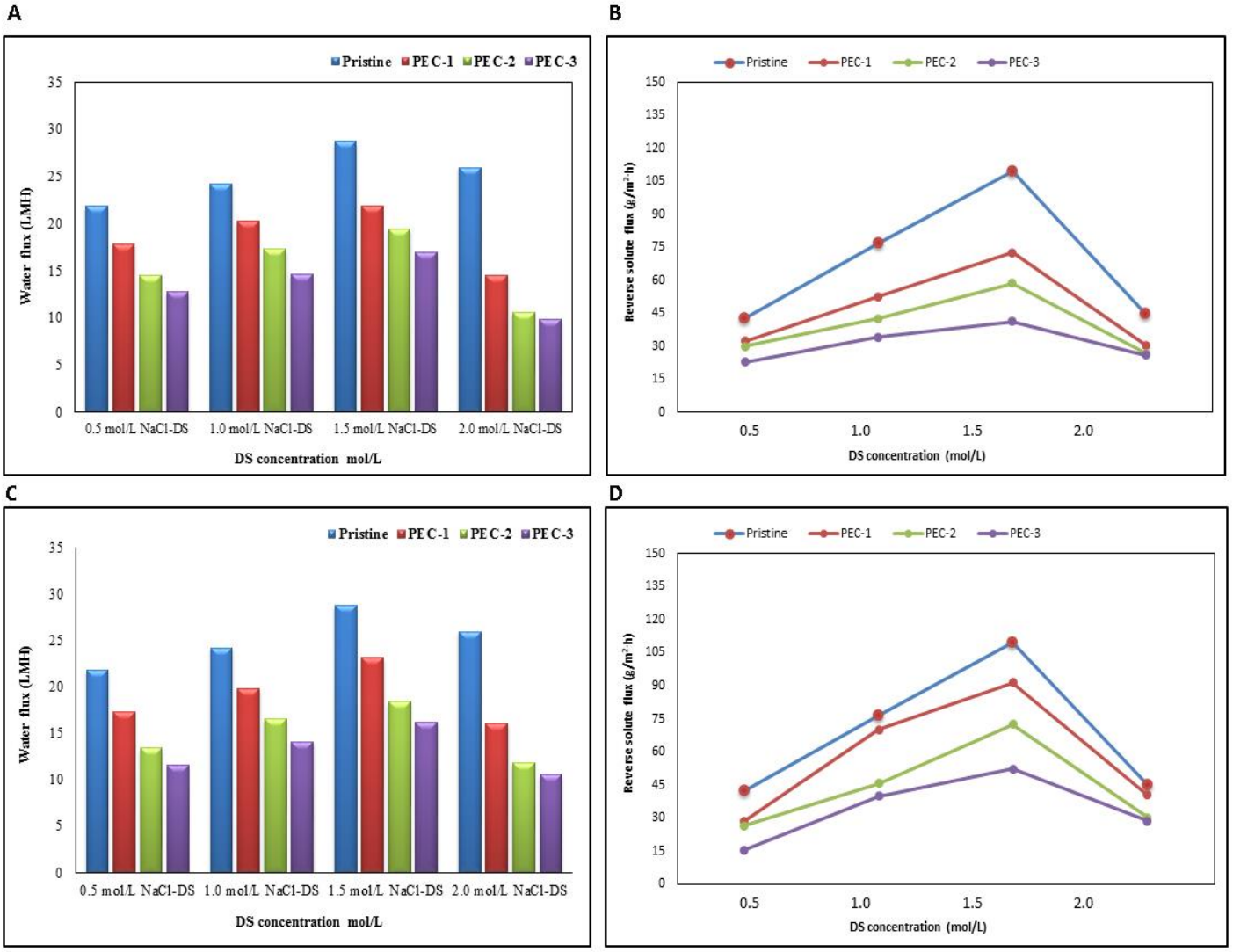

Figure.6 (a, b): The water flux and reverse solute flux of membranes coated with 0.1 MPDADMAC: 0.001 MCMCNa + 0.1 PSS bilayers (PEC-1, PEC-2, PEC-3) when using 0.5, 1.0, 1.5,

2.0 mol/L NaCl DS and DI water FS. (c, d) The water flux and reverse solute flux of membranes coated with 0.1 MPDADMAC: 0.01 MCMCNa + 0.1 PSS bilayers (PEC-1, PEC-2, PEC-3) under the same conditions.

3.6 Determination of the optimal A and B values

The optimum number of bilayers deposited on the PES substrate was chosen based on the membrane transport intrinsic parameters. A semiempirical relationship between the water permeability and solute permeability was obtained as explained above. The pure water permeability and solute permeability were measured to explore the effect of applying multilayer polyelectrolyte to the substrate. Fig.7 demonstrates that the A and B values were decreased significantly when more polyelectrolyte layers were applied on the substrate for both mixing ratios. The membrane coated 2.5 bilayers-M2 generated lower A and B values. As a result of an increase in the viscosity of the PEC solution creating a thicker selective layer reducing the diffusion rate of water across the membrane. Increasing the deposition cycle of polyelectrolytes also led to a thicker selective layer impacting the membrane performance. It is also possible that some polyelectrolyte penetrated or accumulated in the sublayer pores leading to collapse of the pore size, which increased the membrane resistance [40].

Finally, the research findings suggested that the optimum A and B values were 23.1 L m^{-2} h^{-1} bar^{-1} and 1.54 L m^{-2} h^{-1} respectively. Therefore, the optimum number of bilayers was 2.5 containing a mixing ratio of 0.1 M_{PDAMAC}: 0.001 M_{CMCNa} PEC plus 0.01 M PSS polyelectrolyte.

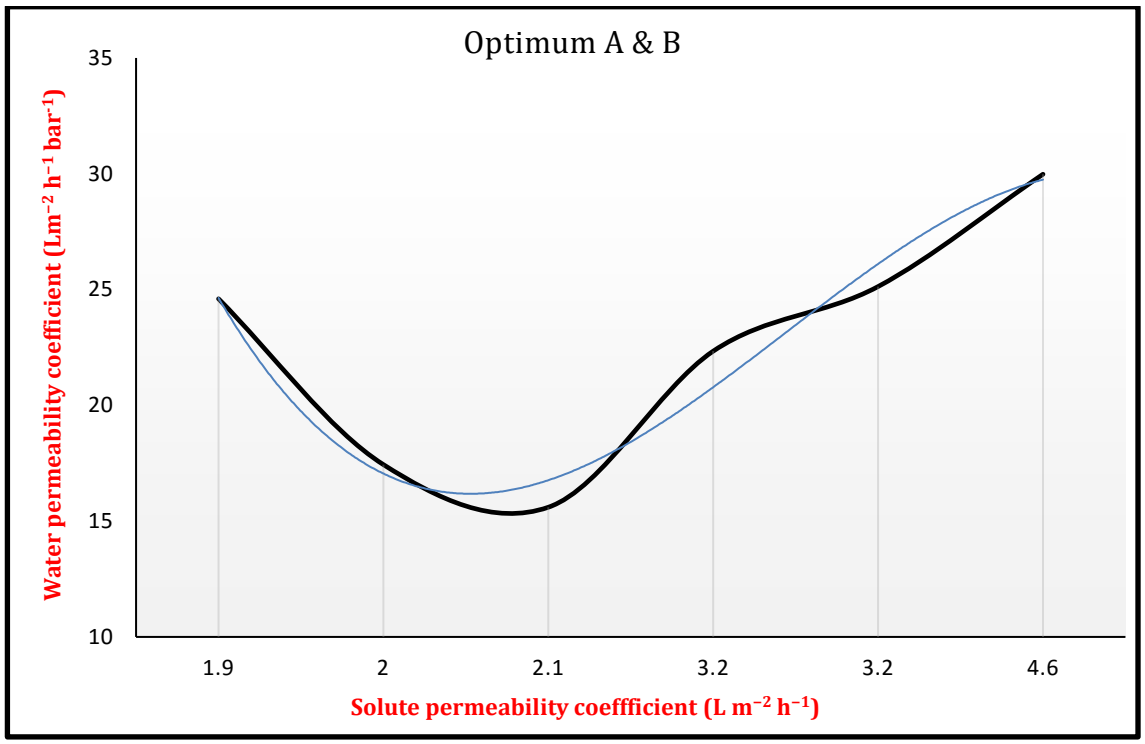

Figure.7: Plot of water permeability coefficients (A) against solute permeability coefficients (B) for all the altered membranes. A and B were computed based on a theoretical model to determine the membrane intrinsic transport characteristics (A and B) that was reported by Tiraferri [27].

4Conclusions

In this research, the surface of PES membranes was tailored by simple LBL technique to fabricate an effective separation layer and enhance the FO membrane performance. ATR-FTIR results indicated that the crosslinking in the PEC solution, the cationic, and anionic polyelectrolytes through using the LBL method was deposited effectively on the substrate. Also, the presence of both polyelectrolytes was confirmed on the altered substrate. SEM surface characterization revealed that the selective layer was homogenous and smooth, which produced acceptable performance with regards to water flux and reverse solute flux. Although

there was a sharp decrease in the mean pore size of the altered substrates, the separation performance was still acceptable. Zeta potential measurements showed that the addition of multilayers of polyelectrolytes increased the positive charges on the substrate. This means that the membrane was highly positive which is desirable to minimize the reverse solute flux of positively charge ions.

The influence of curing temperature and time on membrane performance was observed and the best preparation conditions were selected. To evaluate its potential use as a selective layer, the membrane produced under these conditions was operated in FO process using various concentrations of NaCl as a DS and DI water as a FS. Through using the optimization model developed in the current research, it was possible to identify the optimal water permeability coefficient (A) and solute permeability coefficient (B) of the FO membranes. Also, this optimization model allowed the identification of the optimal thermal treatment and curing time which were 60 ^{O}C and four hours' duration. This fabricated selective layer achieved significant low reverse solute flux at the expense of water permeation.

The mathematical model developed in the current research can be used to predict the optimal A and B values of the FO membrane. This model provided important insight into the membrane performance and the modification procedure. Thus, the optimum A and B values obtained were 23.1 L m^{-2} h^{-1} bar^{-1} and 1.54 L m^{-2} h^{-1} respectively. This allowed the selection of optimum number of PEC bilayers which was found to be 2.5 bilayer including a mixing ratio of 0.1 M_{PDAMAC}: 0.001 M_{CMCNa} PEC. To further maximize the altered membrane performance, it is highly recommended to tailor the PES sublayer structure aiming to reduce the structural parameter and the microporosity. This is because the S parameter was seen to be the most influential on the water flux reduction. The new selective layer exhibited good mechanical integrity and enhanced selectivity hence, this modification approach is of

interest from a particle point of view and could be potential for forward osmosis application. Since the described LBL strategy in this research is easy to scale up, eco-friendly, and cost-effective, it promotes a promising guide to modulating a suitable FO membrane for practical applications in brackish water desalination.

Acknowledgments

This work was supported by Qatar Foundation for Education, Science and Community Development.

References

[1] Nizar, M.M., Norfazliana, Mohamad, A., Z.M.P., Mukhlis, R.A., Khairul, H.A., Azian, A., Mohd, H.D.O., Juhana, J., Ismail, A.F., 2018. Synthesis and performance evaluation of zeolitic imidazolate framework-8 membranes deposited onto alumina hollow fiber for desalination, Korean J. Chem. Eng. pISSN: 0256-1115, DOI: 10.1007/s11814-018-0214-6.

[2] W.A. Suwaileh, D.J. Johnson, S. Sarp, N. Hilal, Advances in forward osmosis membranes: Altering the sub-layer structure via recent fabrication and chemical modification approaches, Desalination. 436 (2018) 176–201

[3] R. Deng, L. Xie, H. Lin, J. Liu, W. Han, Integration of thermal energy and seawater desalination, Energy. 35 (2010) 4368–4374

[4] A. Rahimpour, S.S. Madaeni, A.H. Taheri, Y. Mansourpanah, Coupling TiO2 nanoparticles with UV irradiation for modification of polyethersulfone ultrafiltration membranes, Journal of Membrane Science. 313 (2008) 158–169.

[5] L. Zou, I. Vidalis, D. Steele, A. Michelmore, S.P. Low, J.Q.J.C. Verberk, Surface hydrophilic modification of RO membranes by plasma polymerization for low organic fouling, Journal of Membrane Science. 369 (2011) 420–428.

[6] D. Saeki, M. Imanishi, Y. Ohmukai, T. Maruyama, H. Matsuyama, Stabilization of layer-by-layer assembled nanofiltration membranes by crosslinking via amide bond formation and

siloxane bond formation, Journal of Membrane Science. 447 (2013) 128–133.

[7] G. Xu, S. Wang, H. Zhao, S. Wu, J. Xu, L. Li, X. Liu, Layer-by-layer (LBL) assembly technology as promising strategy for tailoring pressure-driven desalination membranes, Journal of Membrane Science. 493 (2015) 428–443.

[8] S. Kwon, J.S. Lee, S.J. Kwon, S. Yun, S. Lee, J. Lee, Molecular layer-by-layer assembled forward osmosis membranes, Journal of Membrane Science. 488 (2015) 111–120.

[9] Ch. Qiu, L. Setiawan, R. Wang, Ch.Y. Tang, A.G. Fane, High performance flat sheet forward osmosis membrane with an NF-like selective layer on a woven fabric embedded substrate, Desalination. 287 (2012) 266–270.

[10] Ch. Liu, X. Lei, L. Wang, J. Jia, X. Liang, X. Zhao, H. Zhu, Investigation on the removal performances of heavy metal ions with the layer-by-layer assembled forward osmosis membranes, Chemical Engineering Journal. 327 (2017) 60–70.

[11] S. Wang, J. Cai, W. Ding, Z. Xu, Z. Wang, Bio-inspired aquaporinZ containing double-skinned forward osmosis membrane synthesized through layer-by-layer

assembly, Membranes. 5 (2015) 369–384.

[12] H. Salehi, M. Rastgar, A. Shakeri, Anti-fouling and high water permeable forward osmosis membrane fabricated via layer by layer assembly of chitosan/graphene oxide, Applied Surface Science. 413 (2017) 99–108.

[13] R. R. Gonzales, M. J. Park, L. Tijing, D. S. Han, Sh. Phuntsho, H. K. Shon, Modification of nanofiber support layer for thin tilm composite forward osmosis membranes via layer-by-layer polyelectrolyte deposition. Membranes. 8 (2018) 70.

[14] L. Yang, J. Zhang, P. Song, Z. Wang, Layer-by-Layer Assembly for Preparation of High-Performance Forward Osmosis Membrane, IOP Conf. Series: Materials Science and Engineering. 301 (2018) 012032.[15] Q. Zhao, J. Qian, Q. An, Q. Yang, P. Zhang, A facile route for fabricating novel polyelectrolyte complex membrane with high pervaporation performance in isopropanol dehydration, Journal of Membrane Science. 320 (2008) 8–12.

[16] Y. Ji, Q. An, Q. Zhao, H. Chen, J. Qian, C. Gao, Fabrication and performance of a new type of charged nanofiltration membrane based on polyelectrolyte complex, Journal of Membrane Science. 357 (2010) 80–89.

[17] C. S. Tsay, A. J. Mchugh, Mass transfer modeling of asymmetric membrane formation by phase inversion, Polym Sci Part B: Polym Phys. 28 (1990) 1327.

[18] W. Cheng, C. Liu, T. Tong, R. Epsztein, M. Sun, R. Verduzco, J. Ma, M. Elimelech, Selective removal of divalent cations by polyelectrolyte multilayer nanofiltration membrane: Role of polyelectrolyte charge, ion size, and ionic strength, Journal of Membrane Science. 559 (2018) 98–106.

[19] Q. Zhao, J. Qian, Q. An, Z. Gui, H. Jin, M. Yin, Pervaporation dehydration of isopropanol using homogeneous polyelectrolyte complex membranes of poly (diallyldimethylammonium chloride)/sodium carboxymethyl cellulose, Journal of Membrane Science. 329 (2009) 175–182.

[~~24~~20] Q. Saren, Ch.Q. Qiu, Ch.Y. Tang, Synthesis and Characterization of Novel Forward Osmosis Membranes based on Layer-by-Layer Assembly, Environ. Sci. Technol. 45 (2011) 5201–5208.

[21] J. de Grooth, D.M. Reurink, J. Ploegmakers, W.M. de Vos, K. Nijmeijer, Charged micropollutant removal with hollow fiber nanofiltration membranes based on polycation/polyzwitterion/polyanion multilayers, ACS Appl. Mater. Interfaces. 6 (2014) 17009–17017.

[22] D. Wandera, S.R. Wickramasinghe, S.M. Husson, Modification and characterization of ultrafiltration membranes for treatment of produced water, Journal of Membrane Science. 373 (2011) 178–188.

[23] W. Suwaileh, D. Johnson, N. Hilal, Brackish water desalination for agriculture: Assessing the performance of inorganic fertilizer draw solutions, Desalination. 456 (2019) 53–63.

[24] Y. Li, Sh. Huang, Sh. Zhou, A.G. Fane, Y. Zhang, Sh. Zhao, Enhancing water permeability and fouling resistance of polyvinylidene fluoride membranes with

carboxylated nanodiamonds, J. Membr. Sci. 556 (2018) 154–163.

[25] M. N. Chai, M.I.N. Isa, The oleic acid composition Effect on the Carboxymethyl Cellulose Based Biopolymer Electrolyte, Journal of Crystallization Process and Technology. 3 (2013) 1-4.

[26] Y. Baek, J. Kang, P. Theato, J. Yoon, Measuring hydrophilicity of RO membranes by contact angles via sessile drop and captive bubble method: a comparative study, Desalination. 303 (2012) 23–28.

[27] X. Jin, J. Shan, C. Wang, J. Wei, Ch. Y. Tang, Rejection of pharmaceuticals by forward osmosis membranes, J. Hazard. Mater. 227–228 (2012) 55–61.

[28] A. Tiraferri, N.Y. Yip, A.P. Straub, S.R. Castrillon, M. Elimelech, A method for the simultaneous determination of transport and structural parameters of forward osmosis membranes, J. Membr. Sci. 444 (2013) 523–538.

[29] Z. Wang, J. Tang, Ch. Zhu, Y. Dong, Q. Wang, Z. Wu, Chemical cleaning protocols for thin film composite (TFC) polyamide forward osmosis membranes used for municipal wastewater treatment, J. Membr. Sci. 475 (2015) 184–192.

[30] W. Suwaileh, D. Johnson, S. Khodabakhshi, N. Hilal, Superior cross-linking assisted layer by layer modification of forward osmosis membranes for brackish water desalination, Desalination. 463 (2019) 1–12.

[31] P.V. O'neil, Advanced engineering mathematics, Seventh ed., Cengage learning, USA, 2011.

[32] A. Martin, G. Morales, F. Martinez, R. van Grieken, L. Cao, M. Kruk, Acid hybrid catalysts from poly (styrenesulfonic acid) grafted onto ultra-large-pore SBA-15 silica using atom transfer radical polymerization, J. Mater. Chem. 20 (2010) 8026–8035.

[33] A. Hebeish, S. Sharaf, Novel nanocomposite hydrogel for wound dressing and other medical applications, RSC Adv. 5 (2015) 103036–103046.

[34] J. L. Lutkenhaus, K. McEnnis, P. T. Hammond, Nano- and microporous layer-by-layer assemblies containing linear poly(ethylenimine) and poly (acrylic acid), Macromolecules. 41 (2008)

6047-6054.

[35] A. Alghunaim, B.Z. Newby, Cross-linked polystyrene sulfonic acid and polyethylene glycol as a low-fouling material, colloids surf B Biointerfaces. 140 (2016) 514–522.

[36] H. Susanto, M. Ulbricht, Characteristics, performance and stability of polyethersulfone ultrafiltration membranes prepared by phase separation method using different macromolecular additives, Journal of Membrane Science. 327 (2009) 125–135.

[37] G. Han, S. Zhang, X. Li, N. Widjojo, T. Chung, Thin film composite forward osmosis membranes based on polydopamine modified polysulfone substrates with enhancements in both water flux and salt rejection, Chemical Engineering Science. 80 (2012) 219–231.

[38] D. Emadzadeh, W.J. Lau, T. Matsuura, M. Rahbari-Sisakht, A.F. Ismail, A novel thin film composite forward osmosis membrane prepared from PSf–TiO_2 nanocomposite substrate for water desalination, Chemical Engineering Journal. 237 (2014) 70–80

[39] R.W. Holloway, R. Malto, J. Vanneste, T.Y. Cath, Mixed draw solutions for improved forward osmosis performance, Journal of Membrane Science. 491 (2015) 121–131.

[40] B. Su, T. Wang, Z. Wang, X. Gao, C. Gao, Preparation and performance of dynamic layer-by-layer PDADMAC/PSS nanofiltration membrane, Journal of Membrane Science. 423-424 (2012) 324–331.